THE JOURNAL OF PHYSICAL CHEMISTRY A

Article

pubs.acs.org/JPCA

Electronic Properties of Fluorosulfonyl Isocyanate, FSO_2NCO: A Photoelectron Spectroscopy and Synchrotron Photoionization Study

Angélica Moreno Betancourt,[†] Andrea Flores Antognini,[‡] Mauricio F. Erben,[†] Reinaldo Cavasso-Filho,[§] Shengrui Tong,[∥] Maofa Ge,[∥] Carlos O. Della Védova,[†] and Rosana M. Romano*[,†]

[†]CEQUINOR (UNLP−CONICET, CCT La Plata), Departamento de Química, Facultad de Ciencias Exactas, Universidad Nacional de La Plata, CC 962, La Plata (CP 1900), Argentina

[‡]INQUINOA (CONICET-UNT) Instituto de Química Física, Facultad de Bioquímica, Química y Farmacia, Universidad Nacional de Tucumán, San Lorenzo 456, (4000) Tucumán, Argentina

[§]Universidade Federal do ABC, Rua Catequese, 242, CEP: 09090-400, Santo André, São Paulo, Brazil

[∥]State Key Laboratory for Structural Chemistry of Unstable and Stable Species, Beijing National Laboratory for Molecular Sciences (BNLMS), Institute of Chemistry, Chinese Academy of Sciences, Beijing 100190, People's Republic of China

Supporting Information

ABSTRACT: The electronic properties of fluorosulfonyl isocyanate, FSO_2NCO, were investigated by means of photoelectron spectroscopy and synchrotron based techniques. The first ionization potential occurs at 12.3 eV and was attributed to the ejection of electrons formally located at the π NCO molecular orbital (MO), with a contribution from nonbonding orbitals at the oxygen atoms of the SO_2 group. The proposed interpretation of the photoelectron spectrum is consistent with related molecules reported previously and also with the prediction of OVGF (outer valence green function) and P3 (partial third order) calculations. The energy of the inner- and core−shell electrons was determined using X-ray absorption, measuring the total ion yield spectra, and the resonances before each ionization threshold were interpreted in terms of transitions to vacant molecular orbitals. The ionic fragmentation mechanisms in the valence energy region were studied using time-of-flight mass spectrometry as a function of the energy of the incident radiation. At 13 eV the M^+ was the only ion detected in the photoion−photoelectron−coincidence spectrum, while the FSO_2^+ fragment, formed through the breaking of the S−N single bond, appears as the most intense fragment for energies higher than 15 eV. The photoion−photoion−photoelectron−coincidence spectra, taken at the inner- and core-levels energy regions, revealed several different fragmentation pathways, being the most important ones secondary decay after deferred charge separation mechanisms leading to the formation of the O^+/S^+ and C^+/O^+ pairs.

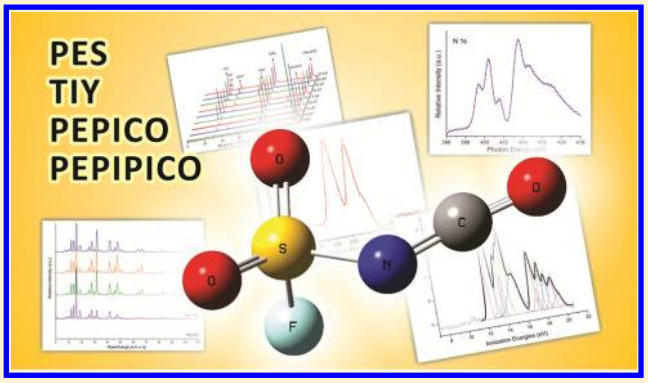

INTRODUCTION

Fluorosulfonyl isocyanate, FSO_2NCO, is an interesting reactant used in different industrial applications, for example, the synthesis of polymers,[1] herbicides, and fungicides.[2] Addition reactions to carbon−nitrogen double bond[3] and cycloaddition to olefins to give β-lactams,[4] among other reactions known for a long time, transform FSO_2NCO into a very versatile and useful reactant.

In a recent investigation our research group has reported matrix-isolation studies on fluoro- and chlorosulfonyl isocyanates, FSO_2NCO and $ClSO_2NCO$, exposed to radiation in the energy range between 800 and 200 nm (1.5−6.2 eV).[5] In contrast to the behavior observed for $ClSO_2NCO$, that decomposes completely to give a 1:1 molecular complex between SO_2 and ClNCO, FSO_2NCO have revealed to be almost photostable in these conditions, with the only formation of FNCO and CO in very small proportions, detected by Fourier transform infrared (FTIR) spectroscopy of the Ar-isolated species. As far as we know, studies using more energetic ionizing light were not previously reported for these molecules.

The structural and conformational properties of fluorosulfonyl isocyanate were determined from gas electron diffraction analysis (GED)[6] and vibrational studies.[7] The GED experiments were interpreted by the presence of only one conformer possessing C_1 structure, with the N═C═O group eclipsed to one of the S═O double bonds.[6] IR and Raman spectra were also consistent with only one conformer, both in the gaseous and liquid phases.[7]

Received: July 16, 2013
Revised: August 12, 2013
Published: August 27, 2013

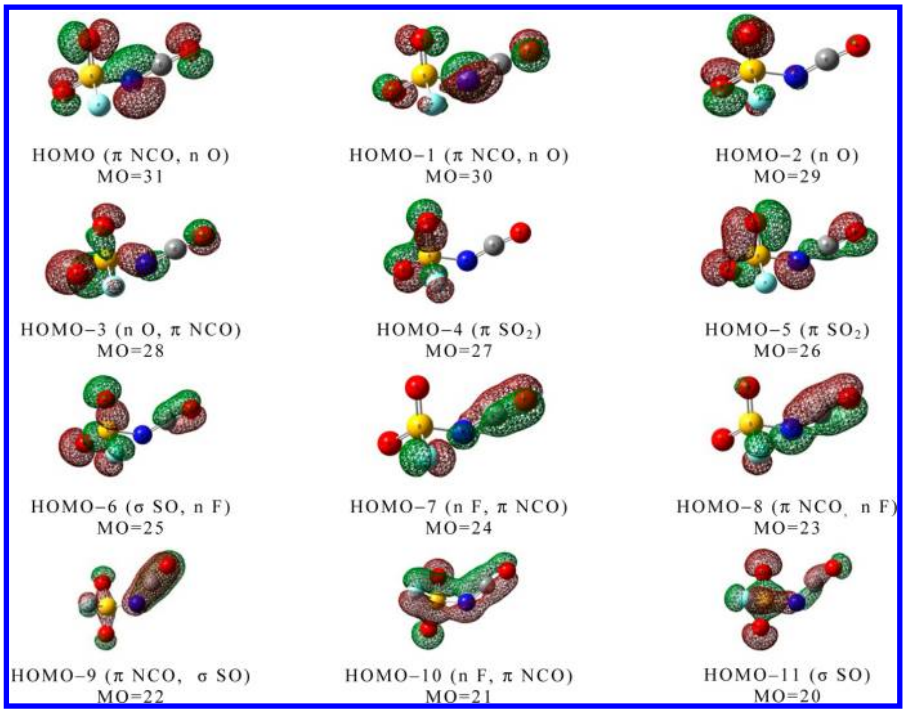

Figure 1. Schematic representation and approximate assignment of the 12 highest occupied molecular orbitals of FSO_2NCO calculated with the OVGF/6-311+G(d,p) approximation.

In this paper we present the study of the electronic properties of FSO_2NCO combining HeI photoelectron spectroscopy with X-ray absorption techniques using tunable synchrotron radiation. Photoelectron spectra, in which the ejected electrons are recorded according with their kinetic energies, contain information about the energies and properties of the outermost valence molecular orbitals (HOMOs). The total ion yield (TIY) spectra taken with tunable synchrotron light, in the range between 100 and 1000 eV, provide the ionization energies of inner and core electrons. Resonance signals below ionization edges can be interpreted in terms of transitions between inner or core electrons and virtual unoccupied molecular orbitals (LUMOs). From this combined approach, it is then possible to gain insights about the valence molecular orbitals, important to interpret chemical bonding, virtual molecular orbitals, relevant in the reactivity properties of a molecule, and inner and core orbitals.

Photofragmentation mechanisms after single and double ionization were also studied using coincidence techniques. In the valence region only single charged species are expected, and the ejected electron and the positive charged ion produced after the fragmentation were detected in coincidence. The fragmentation mechanisms were studied as a function of the incident radiation energy. After inner and core shell electron ionization, the formation of a double charged molecular ion is expected. In this case, the fragmentations usually generate two single charge fragments and also neutral fragments. From the analysis of the shape and slope of the signals detected in the coincidence spectra, the dynamics of the fragmentation can be inferred.

EXPERIMENTAL SECTION

Sample Preparation. FSO_2NCO was obtained through the reaction of $ClSO_2NCO$ with SbF_3 (both Aldrich) and subsequently purified by repeated trap-to-trap distillations under vacuum conditions.[7] The purity of the compounds was checked by means of the FTIR (vapor) and Raman (liquid) spectra.

Photoelectron Spectroscopy. The photoelectron spectrum was recorded on a double-chamber UPS-II machine, which was designed specifically to detect transient species as described elsewhere,[8,9] at a resolution of about 30 meV indicated by the standard $Ar^+(^2P_{3/2})$ photoelectron band. Ionization is provided by single-wavelength HeI radiation. Experimental vertical ionization energies were calibrated with methyl iodide.

Synchrotron Experiments. The synchrotron radiation was used at the Laboratório Nacional de Luz Síncrotron (LNLS), Campinas, Sao Paulo, Brazil.[10] Linearly polarized light monochromatized by a toroidal grating monochromator (TGM beamline, from 12 to 310 eV) or a spherical grating monochromator (SGM beamline, from 200 to 1000 eV)[11] intersects the effusive gaseous sample inside a high-vacuum experimental station[12] at a base pressure in the range of 10^{-8} mbar. During the experiments, the pressure was maintained below 2×10^{-6} mbar. The resolving power is better than 400 in the TGM beamline at the LNLS, being the photon energy resolution from 12 to 21.5 eV given by $E/\Delta E = 550$. Energy calibration in the S 2p energy region was established by means of the S $2p \rightarrow 6a_{1g}$ and S $2p \rightarrow 2t_{2g}$ absorption resonances in SF_6.[13] In the SGM beamline the resolution is $\Delta E/E < 200$. The intensity of the emergent beam was recorded by a light-sensitive diode. The ions produced by the interaction of the gaseous sample with the light beam were detected by means of a time-of-flight (TOF) mass spectrometer of the Wiley−McLaren type for both PEPICO (photoelectron−photoion−coincidence) and PEPIPICO (photoelectron−photoion−photoion−coincidence) measurements.[14,15] This instrument was constructed at the Institute of Physics, Brasilia University, Brasilia, Brazil.[16] The axis of the TOF spectrometer is perpendicular to the photon beam and parallel to the plane

dx.doi.org/10.1021/jp407043c | J. Phys. Chem. A 2013, 117, 9179−9188

of the storage ring. Electrons are accelerated to a MultiChannel Plate (MCP) and recorded without energy analysis. This event starts the flight time determination process for the corresponding ion, which was consequently accelerated to another MCP. High-purity vacuum-ultraviolet photons are used; the problem of contamination by high-order harmonics can be suppressed by the gas-phase harmonic filter recently installed at the TGM beamline at the LNLS.[17−19]

Theoretical Calculations. OVGF (outer valence green function) and P3 (partial third order) calculations using the 6-311+G(d,p) basis set at B3LYP/6-311+G(d,p)-optimized geometry of the most stable conformer have been performed on FSO_2NCO in its ground electronic state using the Gaussian03 program package.[20] The energies of the possible fragments arising from the dissociation of the FSO_2NCO^{+} parent low-lying radical ion were calculated at the UB3LYP/6-311+G(d,p) level of approximation.

RESULTS AND DISCUSSION

Photoelectron Spectroscopy. To help in the interpretation and assignment of the experimental photoelectron spectra, theoretical calculations were performed to obtain the ionization energies and also the character of the molecular orbitals involved in the ionizations. The calculations were carried out with the OVGF and P3 methods, together with the 6-311+G(d,p) basis set, on the molecular structure optimized at the B3LYP/6-311+G(d,p) level. The geometrical parameters obtained by electron diffraction studies[6] were employed as input for the optimization. Figure 1 depicts a schematic representation and approximate assignment of the 12 highest occupied molecular orbital of FSO_2NCO, and Table 1 lists the calculated first vertical ionization energies, together with the experimental values.

Table 1. Experimental Vertical Ionization Energies (IP in eV) of FSO_2NCO, Theoretical Vertical Ionization Energies (E_v in eV) Calculated at OVGF/6-311+G(d,p) and P3/6-311+G(d,p) Levels of Approximation, and Molecular Orbital Characters for FSO_2NCO

	E_v (eV)			
IP (eV)	OVGF/6-311+G(d,p)	P3/6-311+G(d,p)	MO	character
12.3	12.44	12.88	31	π NCO, n O (SO_2)
12.6	12.57	13.15	30	π NCO, n O (SO_2)
13.4	13.22	13.31	29	n O (SO_2)
13.8	14.03	14.22	28	n O (SO_2), π NCO
14.1	14.97	15.03	27	π SO_2
15.0	15.10	15.36	26	π SO_2
16.8	16.74	16.88	25	σ SO, n F
17.2	17.54	17.78	24	n F, π NCO
17.6	17.69	17.85	23	π NCO, n F
18.1	17.72	17.98	22	π NCO, σ SO
18.7	18.86	18.88	21	n F, π NCO
19.3	19.30	19.36	20	σ SO

Figure 2 shows the average of nine He I photoelectron spectra of vapor FSO_2NCO, taken subsequently in the same experimental conditions, to increase the signal-to-noise ratio. As illustrated in the figure, the spectrum is composed of overlapped peaks, corresponding to ionization from different

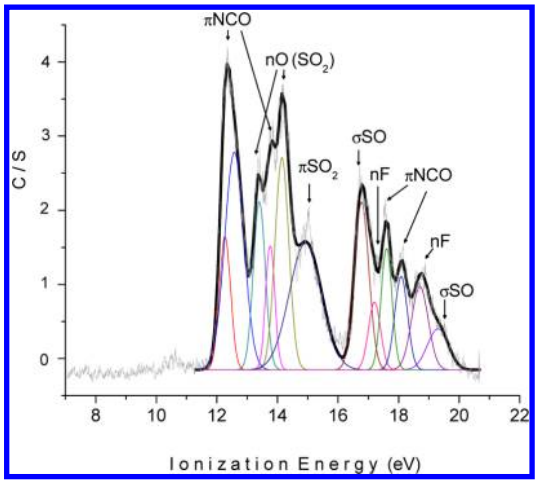

Figure 2. He I photoelectron spectrum of FSO_2NCO (gray trace) and individuals peaks after deconvolution of the spectrum.

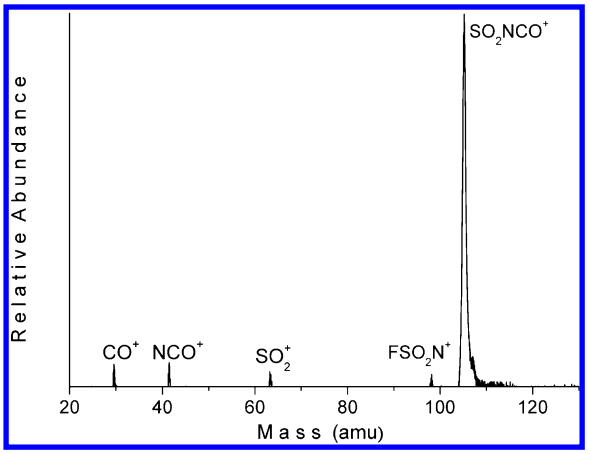

Figure 3. He(I) photoionization mass spectrum (PIMS) of FSO_2NCO.

valence electrons. Individuals peaks were obtained after iterative deconvolution of the spectrum, using Gaussian function and variable bandwidth. The experimental ionization energies (IP in eV), listed in Table 1, were obtained at the maxima of each of the deconvoluted peaks, also depicted in Figure 2.

The first band in the photoelectron spectrum is proposed to be composed by two very close peaks, at approximately 12.3 and 12.6 eV. According to the results of the OVGF and P3 calculations, these bands were attributed to ionization from electrons formally located at the π NCO MO, with a contribution from nonbonding orbitals at the oxygen atoms of the SO_2 group. As shown in Figure 1, the HOMO and HOMO-1 orbital can be considered as a π nonbonding orbital located at the NCO group. The proposed assignment is in complete agreement with the photoelectron spectra previously reported for molecules containing the NCO group (see Table S1),[21−30] that assigned bands in the 9.6−12.6 eV energy range to ionizations of electrons located at the nonbonding π NCO MO. Particularly, the first ionization potential of $ClSO_2NCO$, occurring at 12.02 eV, was also assigned to the same MO.[27]

The third and fourth bands of the spectrum, observed at 13.4 and 13.8 eV, are proposed to arise from nonbonding electrons of the oxygen atoms of the SO_2 group. These values are comparable with the 13.82 eV bands assigned to the removal of electrons from nonbonding oxygen orbitals in the photo-

dx.doi.org/10.1021/jp407043c | J. Phys. Chem. A 2013, 117, 9179−9188

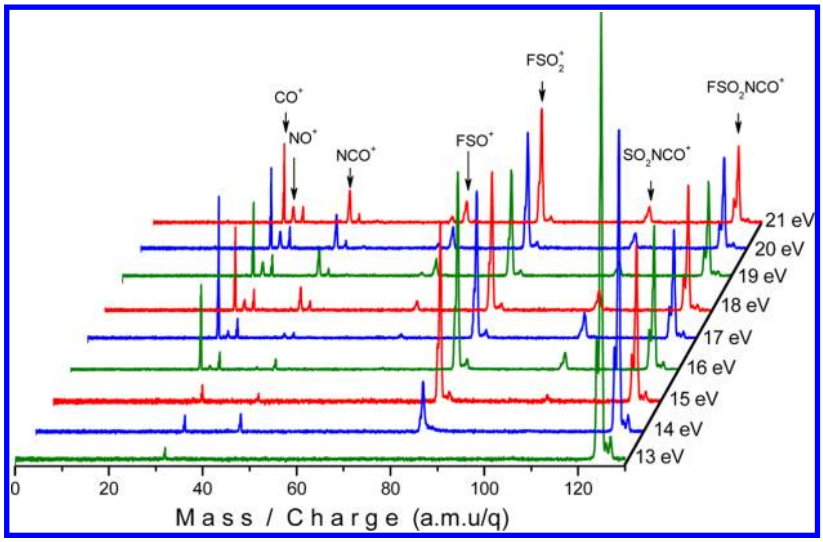

Figure 4. PEPICO spectra of FSO_2NCO measured at different irradiation synchrotron light between 13 and 21 eV.

Table 2. Branching Ratios (%) for Fragment Ions Extracted from PEPICO Spectra as a Function of the Photon Energies between 13 and 21 eV for FSO_2NCO

		photon energy (eV)								
m/z	ion	13	14	15	16	17	18	19	20	21
28	CO^+				12.4	19.2	11.6	11.5	10.8	11.6
30	NO^+				2.0	3.3	4.7	7.2	7.2	7.0
42	NCO^+					3.0	6.7	8.6	9.5	9.9
44	CS^+		7.5	4.2	1.8	1.6	3.6	2.9	3.6	2.5
64	SO_2^+							4.3	4.0	5.0
67	FSO^+					3.2	5.1	7.8	8.8	9.3
83	FSO_2^+		19.2	45.4	45.7	35.0	33.1	26.0	28.6	28.0
106	SO_2NCO^+			9.8	5.8	8.8	8.6	8.0	7.6	8.0
125	FSO_2NCO^+	100.0	73.3	40.6	32.3	25.9	26.6	23.7	19.9	18.7

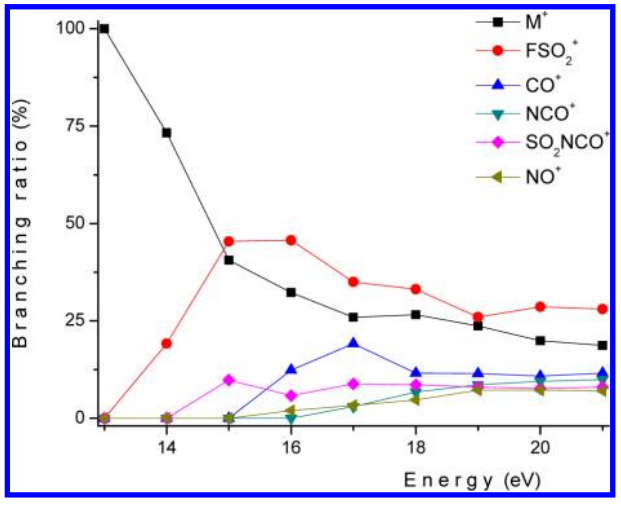

Figure 5. Branching ratios (%) for fragment ions extracted from PEPICO spectra as a function of the photon energies between 13 and 21 eV for FSO_2NCO.

Scheme 1. Relative Energies for Different Possible Fragments of FSO_2NCO^+ Calculated with the UB3LYP/6-311+G(d) Approximation

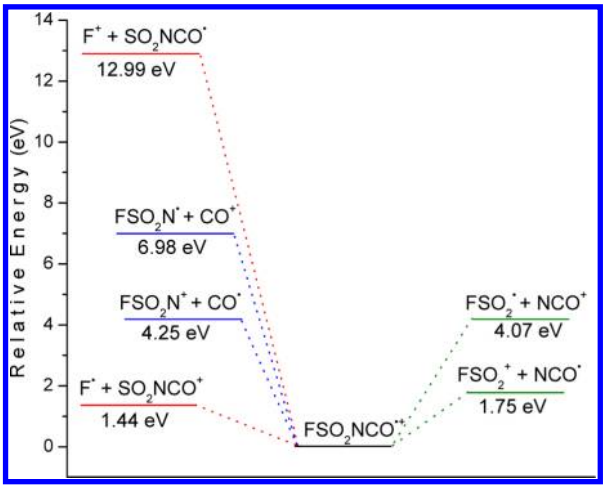

electron spectra of $ClSO_2NCO$ and $ClSO_2N_3$ and the band at 14.00 eV in the spectrum of Cl_2SO_2.[27] The first two vertical ionization potentials of F_2SO_2, reported at 13.55 and 13.81 eV, were also assigned to the same molecular orbitals.[31]

Peaks at 14.1 and 15.0 eV can be assigned to ionizations of π electrons located at the SO_2 group, according with the prediction of OVGF and P3 calculations (see Figure 1). These values are slightly below the reported ones for SO_2, X_2SO, and X_2SO_2, with X = F, Cl, observed in the 16.0−18.4 eV energy range (see Table S2).[31]

Above 16 eV, the photoelectron spectrum was deconvoluted into six bands. The computed calculations predict also six ionizations in this energy region (see Table 1). As can be

dx.doi.org/10.1021/jp407043c | J. Phys. Chem. A 2013, 117, 9179−9188

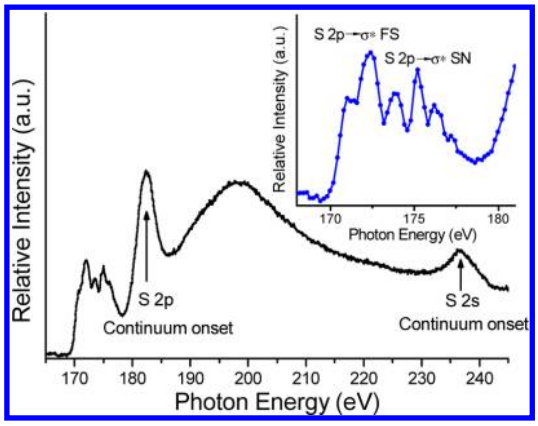

Figure 6. TIY spectrum of FSO_2NCO in the S 2p and S 2s energy region.

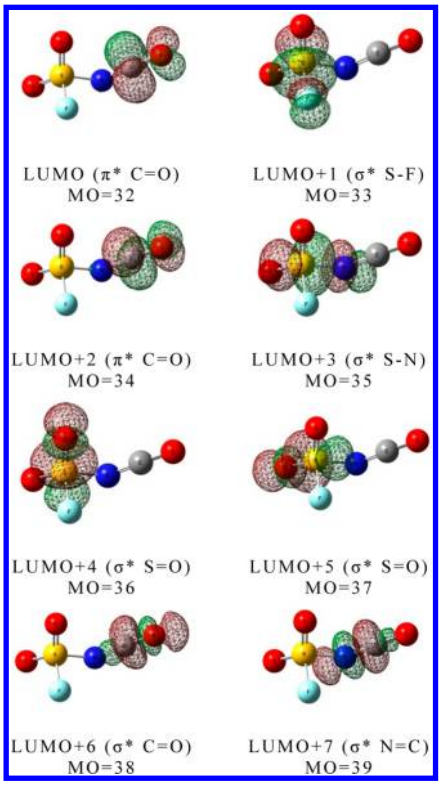

Figure 7. Schematic representation and approximate assignment of the eight lowest unoccupied molecular orbitals of FSO_2NCO.

observed in Figure 1, the characters of these six molecular orbital (from HOMO-6 to HOMO-11) cannot be clearly assigned, since they appear as combinations of different molecular orbitals: two corresponding to nonbonding fluorine atoms, two with bonding π character located at the NCO group, and two arising from the σ SO bonds. The experimental bands in this region were then tentatively assigned, as presented in Table 1. These values are also in agreement with the reported ones for related molecules. Ionizations of nonbonding F electrons were reported between 14.5 and 19.7 eV, some examples being compiled in Table S3.[31−34] Molecular orbitals with bonding π NCO character were assigned to ionizations in the range of 15.85−16−45 eV for the series $Cl_xB(NCO)_{3-x}$, x = 0, 1, 2,[24] and $F_xB(NCO)_{3-x}$, x = 1, 2.[25]

Photoionization Mass Spectroscopy. The He I photoionization mass spectrum (PIMS) of FSO_2NCO, measured together with the photoelectron spectrum, is depicted in Figure 3. As can be observed in the figure, the spectrum is dominated by a strong signal at m/z = 106, corresponding to the SO_2NCO^+ fragment. Peaks at m/z = 97, 64, 42, and 28, attributable to FSO_2N^+, SO_2^+, NCO^+, and CO^+, respectively, were observed with very low intensity. Although the molecular ion is not detected in the spectrum, the identity of the sample is corroborated from the observed ionic fragments. The calculated energy differences of the possible ionic fragments are in agreement with the experimental observation, as it will be presented below in this paper.

Photoionization and Photofragmentation with Synchrotron Radiation in the Valence Energy Region. A low-pressure gaseous beam of FSO_2NCO was exposed to synchrotron monochromatic radiation in the range between 11 and 21 eV. The electrons and the positive ions formed after ionization of the sample were detected by a photoelectron−photoion−coincidence (PEPICO) technique. Taking into account that the pressure of the gaseous beam was maintained below 2×10^{-6} mbar, the results were interpreted in terms of unimolecular processes.

The PEPICO spectra taken at different photon energy are presented in Figure 4, while Table 2 compiles the branching ratios (%) as a function of the incident radiation energy (only fragment that contribute with more than 0.1% were included in the table). The branching ratios of the most abundant fragments were plotted against the irradiation time; the results are shown in Figure 5.

When the sample is irradiated with 13 eV light, just above the first ionization potential, only the molecular ion is observed, denoting the high stability of FSO_2NCO^+ in these conditions and the absence of further accessible photoevolutive states. At 14 eV, the FSO_2^+ fragment is produced and remains as the most abundant photofragment in the whole energy range investigated in the valence region. From 15 to 21 eV this ion presents approximately the same branching ratio than the M^+, as depicted in Figure 5. The breaking of the S−N bond appears then as the most important unimolecular fragmentation mechanism of FSO_2NCO in the valence energy region:

$$FSO_2NCO^+ \rightarrow FSO_2^+ + NCO\cdot$$

The ion arising from the F−S bond breaking, SO_2NCO^+, is observed to appear in the PEPICO spectrum when the sample is excited with 15 eV energy radiation, and maintained an approximately constant relative abundance, below 10%, as the excitation energy increases. CO^+ and NCO^+ fragments were also observed to develop from irradiation energies of 16 eV. The NO^+ ion, that also started to appear at 16 eV, could be formed only by a rearrangement process after ionization.

The energy differences between possible fragments and the molecular ion were calculated with the UB3LYP/6-311+G(d,p) theoretical approximation. Only fragmentations originated in the rupture of only one bond were considered. A schematic representation of the energy profile is presented in Scheme 1. The theoretical relative stabilities of the fragments are qualitatively in agreement with the charged fragments detected in the PEPICO and PIMS spectra. Particularly, the fragmentation of M^+ in SO_2NCO^+ and F· was found as a pathway energetically most favored, in accordance with the most intense ion detected in the PIMS spectrum. The theoretical predictions are also useful for the explanation of the PEPICO spectra variation with the increase of irradiation energy, being the first ions detected FSO_2^+ and SO_2NCO^+, that

dx.doi.org/10.1021/jp407043c | J. Phys. Chem. A 2013, 117, 9179−9188

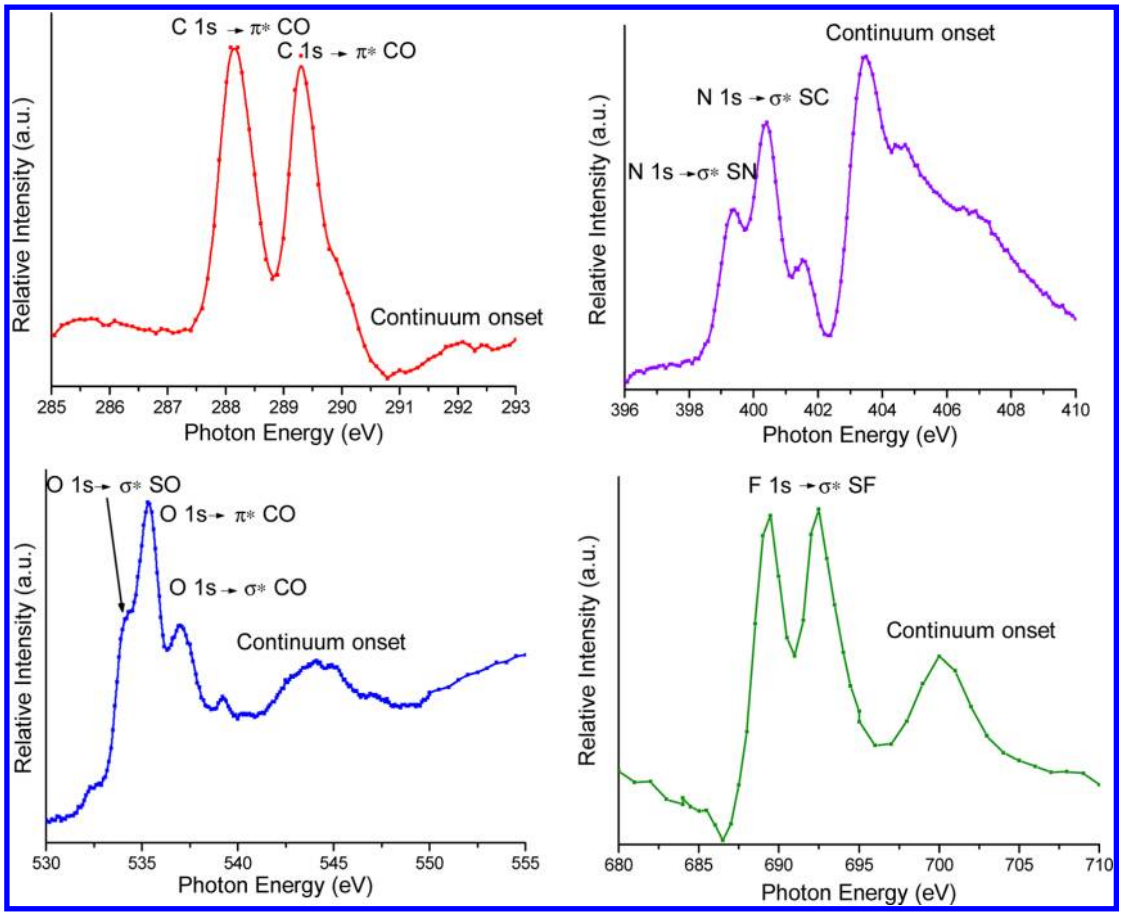

Figure 8. TIY spectra of FSO_2NCO in the C 1s, N 1s, O 1s, and F 1s energy regions.

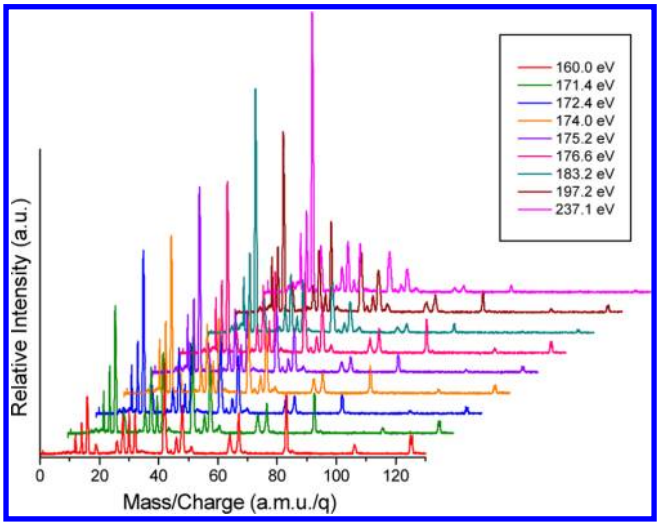

Figure 9. PEPICO spectra of FSO_2NCO measured at different photon energies in the S 2p and S 2s energy regions.

correspond to the fragments generated in the two pathways with lower energy (see Scheme 1).

Photoionization and Photofragmentation with Synchrotron Radiation in the Shallow- and Core-Level Energy Regions. The positive ions produced by photoionization of the sample with radiation between 100 and 1000 eV were detected as a function of the photon energy, without discrimination of the m/q ratio of the ions. Figure 6 presents the average of two TIY spectra of FSO_2NCO between 164 and 245 eV, taken with an energy pass of 0.2 eV, and an acquisition time of 4 s. In this energy region, the ionization of electrons located at the 2p and 2s levels of the S atom is produced. The S 2p and S 2s thresholds are located at approximately 183.0 and 237.1 eV, respectively. Below the S 2p ionization threshold the spectrum is dominated by a group of bands centered at 172.4, 173.8, 175.2, and 176.3 eV and a small shoulders at 171.0 and 177.2 eV, as can be seen in the inset of Figure 6. These resonant signals may be assigned to electronic transitions involving the spin−orbit splitting of the 2p S excited species ($2p_{1/2}$ and $2p_{3/2}$ levels) mainly to the most lower unoccupied π^* and σ^* antibonding molecular orbitals. According with the B3LYP/6-311+G(d,p) calculations, the lowest unoccupied molecular orbital of FSO_2NCO involving the S atom can be assigned to σ^* S−F (LUMO+1), σ^* S−N (LUMO+3), and σ^* S═O (LUMO+4 and LUMO+5). A schematic graphical representation of the eight lowest unoccupied molecular orbital together with an approximately assignment is presented in Figure 7.

Signals arising from the spin−orbit splitting of the S 2p ($2p_{1/2}$ and $2p_{3/2}$) levels are reported to occur with 1.3 eV energy difference in the photoelectron spectrum of the SO_2 molecules.[35] The same energy difference was found in related molecules, as for example dimethyl sulfoxide.[36] Considering not only the 1.3 eV reported energy difference but also the expected 2:1 ratio of the $2p_{3/2}$:$2p_{1/2}$ components, the TIY spectrum of FSO_2NCO (see the inset of Figure 6) can be interpreted as composed mainly for resonances from the S $2p_{3/2}$ and $2p_{1/2}$ levels to two unoccupied molecular orbitals. Tentatively, S2p → σ^* S−F (LUMO+1) and S2p → σ^* S−N

dx.doi.org/10.1021/jp407043c | J. Phys. Chem. A 2013, 117, 9179−9188

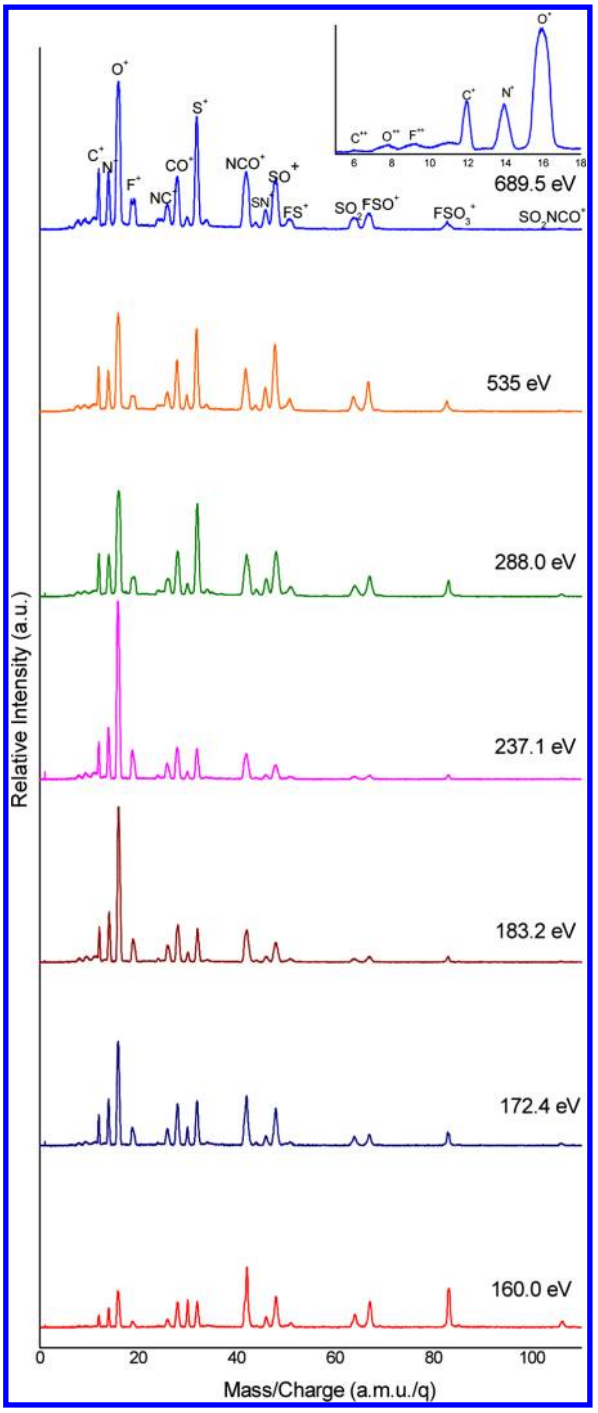

Figure 10. PEPICO spectra of FSO_2NCO measured at different photon energies in the S 2p and 2s, C 1s, O 1s, and F 1s energy regions.

(LUMO+3) transitions could be proposed to explain the two most intense pairs of resonances.

Figure 8 presents the TIY spectra of FSO_2NCO corresponding to the C 1s, N 1s, O 1s, and F 1s energy regions. In the C 1s region, the spectrum shows two signals, at 288.1 and 289.3 eV, that can be attributed to C 1s → π^* C═O (LUMO) and C 1s → π^* C═O (LUMO+2). The ionization threshold of the N 1s electrons is observed at 403.5 eV. The signals below the ionization edge, at 399.4, 400.4, and 401.6 eV, can be associated with N 1s → σ^* S−N (LUMO+3) and N 1s → σ^* N═C (LUMO+7) transitions. Below the O 1s threshold, occurring at approximately 560 eV, a group of signals is observed. The complex resonance pattern, with the most intense peak at 535.3 eV, can be explained through partially overlapping transitions of 1s electrons located in each of the three oxygen atoms of the molecules to different vacant molecular orbitals. Presumably, resonances between O 1s (−SO_2−) → σ^* S═O (LUMO+4, LUMO+5), O 1s (−NCO) → π^* C═O, and O 1s (−NCO) → σ^* C═O are responsible for the observed signals. Considering that signals arising from transitions of O 1s electrons to antibonding molecular orbitals with π character are usually more intense that the ones produced in resonance with σ^* molecular orbitals,[37,38] the most intense feature of the spectrum localized at 535.3 eV was tentatively assigned to the O 1s (−NCO) → π^* C═O transition. The ionization edge of F 1s electrons located at approximately 699.9 eV is preceded by two strong signals at 689.5 and 692.5 eV.

PEPICO spectra of FSO_2NCO were measured at resonant and threshold excitation energies of S 2p, S 2s, C 1s, N 1s, O 1s, and F 1s electrons. The spectra are shown in Figures 9 and 10, and Table 3 lists the positive ion branching ratios (%) as a function of the energy of the incident radiation (only fragments that contribute with more than 0.1% were included in the Table). The fragmentation processes of FSO_2NCO become more important as the irradiation energy increases, since the abundance of the molecular ion is observed to decrease monotonically. Only the lightest ionic fragment arising from a molecular fragmentation is detected in the PEPICO spectra. This means that SO_2^+, FSO^+, FSO_2^+, and FSO_2NCO^+, should be originated from a single ionization processes.

Comparing the branching ratios (%) of the ionic fragments at different ionization energies (Table 3) an increment in the abundances of atomic ions is observed as radiation energy increases, although specific site effects are not evident. The most abundant ion at all the studied energies is O^+, with relative intensities from 13.0% at 160 eV to 41.2% at 237.1 eV. Below the S 2p threshold the NCO^+ ion is the second most abundant fragment of the PEPICO spectra. At higher energies, SO^+, CO^+, and S^+ became also important. When the sample is excited with radiation corresponding to the ionization of 1s electrons, double charged atomic fragments like C^{2+}, O^{2+}, F^{2+}, and SO^{2+} were observed (see Figure 10).

Photofragmentation Mechanisms. The detection of one electron and two positive ions produced from a unimolecular photofragmentation as a consequence of a double photoionization process, known as PEPIPICO (photoelectron−photoion−photoion−coincidence) spectra, is a powerful technique to study photofragmentation mechanisms after double ionization of a molecule. The slope of the coincidence islands of the PEPIPICO spectra contains valuable information of the fragmentation dynamics.

The PEPIPICO spectra of FSO_2NCO were recorded at different energies. The relative intensities of the most abundant coincidences are listed in Table S4 as a function of the ionization energy. The coincidence between O^+ and S^+ was found to be the most intense one for all the studied energies, with the exception of the spectra taken with 600 and 730 eV for which the C^+/O^+ coincidence is the most abundant in the PEPIPICO spectra. Figure 11 shows the PEPIPICO spectrum taken at 182.4 eV and the island for the coincidence between O^+ and S^+, while Figure S1 presents the T_1 and T_2 projection of the spectrum.

Following the formalisms proposed by Eland,[39] the fragmentation mechanisms of FSO_2NCO were investigated,

dx.doi.org/10.1021/jp407043c | J. Phys. Chem. A 2013, 117, 9179−9188

Table 3. Branching Ratios (%) for Fragment Ions Extracted from PEPICO Spectra of FSO_2NCO as a Function of the Photon Energies between in the S 2p, S 2s, C 1s, O 1s, and F 1s Energy Regions

		photon energy (eV)															
m/z	ion	160.0	171.4	172.4	174.0	175.2	176.6	183.2	197.2	237.1	287.9	288.0	500.0	535.0	600.0	689.5	730.0
6	C^{2+}	0.0	0.0	0.0	0.0	0.0	0.0	0.0	0.0	0.0	0.6	0.7	0.7	0.8	1.1	0.5	1.3
8	O^{2+}	2.6	2.7	2.6	2.5	2.9	2.3	2.8	2.4	2.5	2.2	2.1	2.1	2.6	3.2	1.7	3.4
9.5	F^{2+}	2.8	3.2	3.3	2.7	3.1	2.6	3.4	2.7	3.2	2.3	2.3	1.8	2.7	2.2	1.8	2.3
12	C^+	3.5	4.6	5.3	5.7	6.0	5.7	5.8	5.7	6.3	5.9	5.5	8.0	5.8	10.1	5.6	9.7
14	N^+	5.4	7.5	8.5	8.3	8.9	8.2	9.3	8.2	9.8	6.9	6.9	6.6	6.4	5.3	7.0	5.6
16	O^+	13.0	19.1	24.0	23.2	27.3	25.1	35.6	26.4	40.8	25.4	23.2	30.5	21.5	32.2	23.5	31.2
19	F^+	3.5	4.6	5.3	4.8	5.5	4.9	6.3	5.1	7.4	5.2	5.0	5.1	4.4	3.9	5.1	4.5
22	CS^{2+}	0.0	0.0	0.0	0.0	0.0	0.0	0.0	0.0	0.0	0.3	0.3	0.3	0.3	1.1	0.3	1.0
24	SO^{2+}	0.0	1.0	1.0	1.0	1.1	0.9	1.1	1.0	1.0	1.0	1.0	0.9	1.1	0.8	1.0	0.8
26	NC^+	3.6	4.2	4.4	4.4	4.6	4.5	4.4	4.5	4.0	3.7	3.7	3.1	3.6	2.6	3.7	2.7
28	CO^+	7.3	8.4	8.5	8.6	8.1	8.4	8.2	8.9	7.0	7.3	7.3	6.8	7.4	8.0	7.4	7.4
30	NO^+	5.3	3.6	3.2	3.4	3.1	3.1	2.0	2.2	1.5	1.6	1.8	1.2	2.0	1.1	1.8	1.1
32	S^+	6.7	8.7	8.1	8.3	7.1	8.5	6.0	9.9	5.6	13.0	13.0	12.6	11.7	9.5	13.1	9.9
42	NCO^+	14.4	11.9	10.7	10.1	9.1	9.9	8.1	9.5	6.4	7.5	7.7	6.2	7.2	5.9	7.8	6.2
44	CS^+	1.2	1.1	1.0	1.0	1.1	1.0	0.7	1.0	0.6	0.8	0.8	0.8	0.7	0.6	0.8	0.6
46	SN^+	3.2	2.7	2.3	2.5	2.2	2.3	1.6	2.3	1.3	2.2	2.5	1.8	3.0	1.6	2.5	1.6
48	SO^+	8.7	8.6	7.5	7.6	6.2	6.6	4.7	6.6	3.7	6.9	7.5	5.8	9.4	5.1	7.6	5.2
51	FS^+	2.4	2.0	1.6	1.7	1.8	1.7	1.4	1.7	1.1	1.6	1.8	1.4	1.9	1.3	1.8	1.3
64	SO_2^+	4.3	3.3	2.5	2.5	2.3	2.3	1.5	1.9	1.1	1.7	2.0	1.3	2.3	1.5	2.0	1.5
67	FSO^+	6.1	3.5	2.5	2.8	2.4	2.9	1.6	2.3	1.2	2.5	2.9	2.0	3.7	2.1	3.0	1.8
83	FSO_2^+	7.4	3.2	2.0	2.4	1.9	2.6	1.0	1.6	0.7	1.3	1.6	0.9	1.2	0.7	1.7	0.7
106	SO_2NCO^+	1.6	1.0	0.7	0.7	0.7	0.7	0.4	0.6	0.3	0.2	0.4	0.1	0.2	0.1	0.4	0.2
125	FSO_2NCO^+	2.3	1.0	0.7	0.8	0.7	0.8	0.4	0.5	0.3	0.3	0.4	0.3	0.3	0.1	0.1	0.0

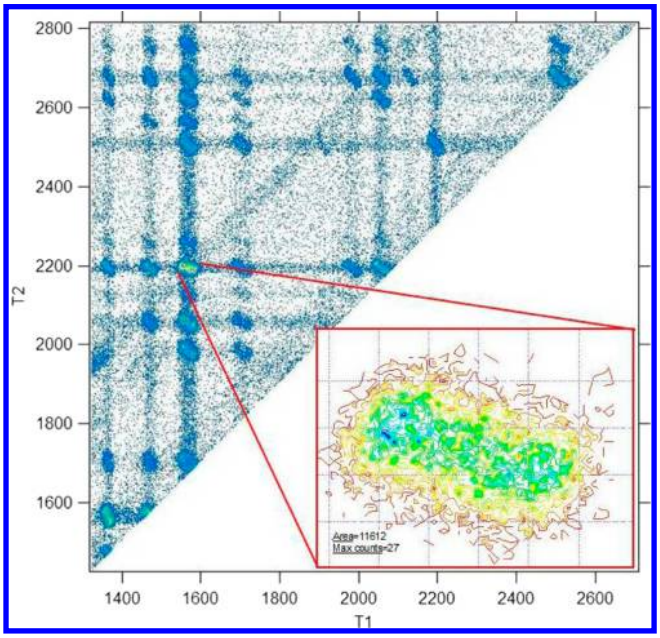

Figure 11. PEPIPICO spectrum of FSO_2NCO measured at 182.4 eV. The inset shows the coincidence island between O^+ and S^+ atomic ions.

by comparison of the experimental slopes and shapes of the coincidences with the calculated for different possible mechanisms. Although for several pairs of ions arriving in coincidence plausible mechanisms could be proposed, as summarized in Table 4, in other cases more than one mechanism could explain the experimental slope of the islands, and they will not be discussed.

Most of the fragmentations channels of FSO_2NCO^{2+} follow a secondary decay after deferred charge separation. The two most abundant coincidences in the PEPIPICO spectra, O^+/S^+ and C^+/O^+, are explainable by this kind of fragmentation mechanisms (see Table 4). Competitive secondary decay sequences are also proposed for the generation of some fragments, as N^+/SO^+, O^+/NCO^+, and CO^+/SO^+.

Eland and co-workers demonstrated that the ejection of a neutral fluorine atom is usually the first step of a DCS dissociation of processes of doubly charged ions from fluorinated compounds.[40] The heaviest ions detected in coincidence, NCO^+ and SO^+, are supposed to arise from a deferred charge separation mechanism.

CONCLUSION

The first ionization potential of fluorosulfonyl isocyanates, FSO_2NCO, was determined by photoelectron spectroscopy at approximately 12.3 eV. According with OVGF and P3 theoretical calculations and the comparison with related molecules, the first two bands of the photoelectron spectrum were attributed to ionization from electrons formally located at the π NCO MO, with a contribution from nonbonding orbitals at the oxygen atoms of the SO_2 group. A complete tentative assignment of the photoelectron spectrum, composed by 12 bands, was proposed based on the prediction of OVGF and P3 calculations and also by the comparison with related molecules.

The excitation and ionization energies around the S 2p, S 2s, C 1s, N 1s, O 1s, and F 1s edges were determined using tunable synchrotron radiation light source. The resonances above the ionization thresholds were interpreted in terms of transitions between core- and inner-shell levels and unoccupied molecular orbitals, with the aid of molecular orbital calculations.

The photofragmentation mechanisms of FSO_2NCO after ionization with light of different energies were investigated. In

dx.doi.org/10.1021/jp407043c | J. Phys. Chem. A 2013, 117, 9179−9188

Table 4. Proposed Fragmentation Mechanisms for FSO_2NCO Induced by 182.4 eV Irradiation

coincidence[a]	%[b]	α_{exp}[c]		proposed mechanisms[d]	α_{theor}[e]
C^+/O^+	9.3	−2.5	SD-DCS	$FSO_2NCO^{2+} \rightarrow FSO_2 + NCO^{2+}$	−2.17
				$NCO^{2+} \rightarrow NC^+ + \mathbf{O^+}$	
				$NC^+ \rightarrow N + \mathbf{C^+}$	
N^+/SO^+	2.1	−1.7	CSD	$FSO_2NCO^{2+} \rightarrow FSO_2^+ + NCO^+$	−1.73
				$FSO_2^+ \rightarrow \mathbf{SO^+}$ + n.f.	
				$NCO^+ \rightarrow CO + \mathbf{N^+}$	
O^+/NC^+	5.6	−0.7	SD-DCS	$FSO_2NCO^{2+} \rightarrow ONCO^{2+}$ + n.f.	−0.62
				$ONCO^{2+} \rightarrow NCO^+ + \mathbf{O^+}$	
				$NCO^+ \rightarrow O + \mathbf{NC^+}$	
O^+/CO^+	7.7	−0.7	SD-DCS	$FSO_2NCO^{2+} \rightarrow ONCO^{2+}$ + n.f.	−0.67
				$ONCO^{2+} \rightarrow NCO^+ + \mathbf{O^+}$	
				$NCO^+ \rightarrow N + \mathbf{CO^+}$	
O^+/S^+	23.0	−0.4	SD-DCS	$FSO_2NCO^{2+} \rightarrow SO_2NCO^{2+} + F$	−0.35
				$SO_2NCO^{2+} \rightarrow OSNCO^+ + \mathbf{O^+}$	
				$OSNCO^+ \rightarrow \mathbf{S^+}$ + n.f.	
O^+/NCO^+	5.3	−1.0	CDS	$FSO_2NCO^{2+} \rightarrow ONCO^{2+}$ + n.f.	−1.00
				$ONCO^{2+} \rightarrow \mathbf{O^+} + \mathbf{NCO^+}$	
O^+/SN^+	3.4	0.6	SD-DCS	$FSO_2NCO^{2+} \rightarrow FSO_2N^{2+}$ + CO	0.57
				$FSO_2N^{2+} \rightarrow FSON^+ + \mathbf{O^+}$	
				$FSON^+ \rightarrow \mathbf{SN^+}$ + n.f.	
CO^+/SN^+	1.7	−0.8	SD-DCS	$FSO_2NCO^{2+} \rightarrow OSNCO^{2+}$ + n.f.	−0.74
				$OSNCO^{2+} \rightarrow OSN^+ + \mathbf{CO^+}$	
				$OSN^+ \rightarrow O + \mathbf{SN^+}$	
CO^+/SO^+	2.6	−1.5	CSD	$FSO_2NCO^{2+} \rightarrow FSO^+ + ONCO^+$	−1.50
				$FSO^+ \rightarrow F + \mathbf{SO^+}$	
				$ONCO^+ \rightarrow NO + \mathbf{CO^+}$	
S^+/NCO^+	2.2	−1.5	SD-DCS	$FSO_2NCO^{2+} \rightarrow OSNCO^{2+}$ + n.f.	−1.50
				$OSNCO^{2+} \rightarrow SO^+ + \mathbf{NCO^+}$	
				$SO^+ \rightarrow \mathbf{S^+} + O$	
NCO^+/SO^+	5.0	−1.0	DCS	$FSO_2NCO^{2+} \rightarrow SO_2NCO^{2+} + F$	−1.00
				$SO_2NCO^{2+} \rightarrow SONCO^{2+} + O$	
				$SONCO^{2+} \rightarrow \mathbf{NCO^+} + \mathbf{SO^+}$	

[a]Ions arriving in coincidence in T_1 and T_2 in the PEPIPCO. [b]Relative intensity. [c]Experimental slope of the coincidence. [d]SD-DCS: secondary decay after deferred charge separation; CSD: competitive secondary decay; DCS: deferred charge separation. n.f.: neutral fragments. Ions in bold type correspond to the fragments detected in coincidence. [e]Theoretical slope calculated with the formalism proposed by Eland (ref 39).

the valence region the most important fragmentation mechanisms of the M^+ occurs through the breaking of the S−N single bond, originating the FSO_2^+ fragment. As the incident energy increases, more fragments are observed to appear, as expected.

In the inner- and core-levels energy regions, several alternative fragmentation mechanisms of the M^{2+} parent double charged ion were produced. The two most important mechanisms lead to the formation of the pairs O^+/S^+ and C^+/O^+, through a secondary decay after deferred charge separation pathway.

■ ASSOCIATED CONTENT

Supporting Information

Comparison of the experimental ionization energies (IP in eV) of electrons assigned to π orbitals located at the NCO group of different molecules (Table S1), comparison of the experimental ionization energies (IP in eV) of electrons assigned to S−O π orbitals in different molecules (Table S2), comparison of the experimental ionization energies (IP in eV) of electrons assigned to nonbonding electrons located at the fluorine atoms in different molecules (Table S3), relative intensities of the coincidences in the PEPIPICO spectra of FSO_2NCO at different ionization energies (Table S4), and T1 and T2 projections of the PEPIPICO spectrum of FSO_2NCO recorded at 182.4 eV. This material is available free of charge via the Internet at http://pubs.acs.org.

■ AUTHOR INFORMATION

Corresponding Author

*E-mail: romano@quimica.unlp.edu.ar.

Notes

The authors declare no competing financial interest.

■ ACKNOWLEDGMENTS

This work has been largely supported by the Brazilian Synchrotron Light Source (LNLS) under Proposals TGM-10926 and SGM-11670. The authors wish to thank Arnaldo Naves de Brito and his research group for fruitful discussions and generous collaboration during their several stays in Campinas and the TGM and SGM beam line staffs for their assistance throughout the experiments. They also are indebted to the Agencia Nacional de Promoción Científica y Tecnológica (ANPCyT), Consejo Nacional de Investigaciones Científicas y Técnicas (CONICET), and the Facultad de Ciencias Exactas, Universidad Nacional de La Plata for financial support.

■ REFERENCES

(1) MacNeill, C. M.; Dai, J.; Day, C. S.; Lazar, S. P.; Howell, S. J.; Noftle, R. E. Synthesis, Structure, and Electrochemistry of N-(3-thenoyl)fluorosulfonimide and bis(2-thenoic)imide. Preparation of Polymers Containing the Fluorosulfonimide Group. *Synth. Met.* **2009**, *159* (15−16), 1628−1635.

(2) Hoerlein, G.; Mildenberger, H.; Kroeniger, A.; Haertel, K. Fungicidal 2-(carbomethoxyamino)-1-(sulfonylcarbamoyl)-benzimidazoles. Ger. Offen. DE 2126838 A 19721214, 1992.

(3) Clauss, v. K. Reaction of Chlorosulfonyl Isocyanate with Olefins. *Justus Liebigs Ann. Chem.* **1969**, *722*, 110−121.

(4) Lattrell, R. Cycloaddition Reactions with α,β-dihetero-substituted Olefins. I. Reactions with Sulfonyl Isocyanates. *Justus Liebigs Ann. Chem.* **1969**, *722*, 132−141.

(5) Robles, N. L.; Flores Antognini, A.; Romano, R. M. Formation of XNCO Species (X = F, Cl) Through Matrix-Isolation Photochemistry of XSO_2NCO Molecules. *J. Photochem. Photobiol., A: Chem.* **2011**, *223*, 194−201.

(6) Della Védova, C. O.; Cutin, E. H.; Mack, H.-G.; Oberhammer, H. Conformation and Gas-Phase Structure of Fluorosulfonyl Isocyanate, FSO_2NCO. *J. Mol. Struct.* **1996**, *380*, 167−170.

(7) Álvarez, R. M. S.; Cutin, E. H.; Mack, H.-G.; Della Védova, C. O. Vibrational and Conformational Study of FSO_2NCO: FT-IR, Pre-Resonance Raman Effect, Force Field and Theoretical Calculations. *J. Mol. Struct.* **1994**, *323*, 29−38.

(8) Yao, L.; Ge, M.; Wang, W.; Zeng, X.; Sun, Z.; Wang, D. Gas-Phase Generation and Electronic Structure Investigation of Chlorosulfanyl Thiocyanate, ClSSCN. *Inorg. Chem.* **2006**, *45*, 5971−5975.
(9) Du, L.; Yao, L.; Zeng, X.; Ge, M.; Wang, D. HeI Photoelectron Spectroscopy and Theoretical Study of Trichloromethanesulfenyl Acetate, $CCl_3SOC(O)CH_3$, and Trichloromethanesulfenyl Trifluoroacetate, $CCl_3SOC(O)CF_3$. *J. Phys. Chem. A.* **2007**, *111*, 4944−4949.
(10) Lira, A. C.; Rodrigues, A. R. D.; Rosa, A.; Gonçalves da Silva, C. E. T.; Pardine, C.; Scorzato, C.; Wisnivesky, D.; Rafael, F.; Franco, G. S.; Tosin, G.; Lin, L.; et al. First Year Operation of the Brazilian Sinchrotron Light Source. *European Particle Accelerator Conference*, Stockholm, Sweden, June 22−26, 1998.
(11) Fonseca, P. T.; Pacheco, J. G.; Samogin, E.; de Castro, A. R. B. Vacuum Ultraviolet Beam Lines at Laboratório Nacional de Luz Síncrotron, the Brazilian Synchrotron Source. *Rev. Sci. Instrum.* **1992**, *63*, 1256−1259.
(12) Burmeister, F.; Coutinho, L. H.; Marinho, R. R. T.; Homem, M. G. P.; de Morais, M. A. A.; Mocellin, A.; Björneholm, O.; Sorensen, S. L.; Fonseca, P. T.; Lindgren, A.; et al. Description and Performance of an Electron-Ion Coincidence TOF Spectrometer Used at the Brazilian Synchrotron Facility LNLS. *J. Electron Spectrosc. Relat. Phenom.* **2010**, *180*, 6−13.
(13) Kivimaki, A.; Alvarez Ruiz, J.; Erman, P.; Hatherly, P.; Melero García, E.; Rachlew, E.; Rius i Riu, J.; Stankiewicz, M. An Energy Resolved Electron−Ion Coincidence Study Near the S 2p Thresholds of the SF_6 Molecule. *J. Phys. B* **2003**, 781−791.
(14) Frasinski, L. J.; Stankiewicz, M.; Randall, K. J.; Hatherly, P. A.; Codling, K. Dissociative Photoionisation of Molecules Probed by Triple Coincidence; Double Time-of-Flight Techniques. *J. Phys. B* **1986**, *19*, L819−L824.
(15) Eland, J. H. D.; Wort, F. S.; Royds, R. N. A Photoelectron-Ion-Ion Triple Coincidence Technique for the Study of Double Photoionization and its consequences. *J. Electron Spectrosc. Relat. Phenom.* **1986**, *41*, 297−309.
(16) Naves de Brito, A.; Feifel, R.; Mocellin, A.; Machado, A. B.; Sundin, S.; Hjelte, I.; Sorensen, S. L.; Björneholm, O. Femtosecond Dissociation Dynamics of Core Excited Molecular Water. *Chem. Phys. Lett.* **1999**, *309*, 377−385.
(17) Cavasso Filho, R. L.; Homem, M. G. P.; Landers, R.; Naves de Brito, A. Advances on the Brazilian Toroidal Grating Monochromator (TGM) Beamline. *J. Electron Spectrosc. Relat. Phenom.* **2005**, *144−147*, 1125−1127.
(18) Cavasso Filho, R. L.; Lago, A. F.; Homem, M. G. P.; Pilling, S.; Naves de Brito, A. Delivering High-Purity Vacuum Ultraviolet Photons at the Brazilian Toroidal Grating Monochromator (TGM) Beamline. *J. Electron Spectrosc. Relat. Phenom.* **2007**, *156−158*, 168−171.
(19) Cavasso Filho, R. L.; Homem, M. G. P.; Fonseca, P. T.; Naves de Brito, A. A Synchrotron Beamline for Delivering High Purity Vacuum Ultraviolet Photons. *Rev. Sci. Instrum.* **2007**, *78*, 115104.
(20) Frisch, M. J.; Trucks, G. W.; Schlegel, H. B.; Scuseria, G. E.; Robb, M. A.; Cheeseman, J. R.; Montgomery, J. A., Jr.; Vreven, T.; Kudin, K. N.; Burant; et al. *Gaussian 03*, Revision B.04; Gaussian, Inc.: Pittsburgh, PA, 2003.
(21) Ma, C. P.; Ge, M. F. Electronic Structure and Photoionization Mass Spectroscopy of Methoxycarbonylsulfenyl Isocyanate, $CH_3OC(O)SNCO$. *J. Mol. Struct.* **2008**, *892*, 68−73.
(22) Cradock, S.; Ebsworth, E. A. V.; Murdoch, J. D. Photoelectron Spectra of Some Group 4 Pseudohalides and Related Compounds. *J. Chem. Soc., Faraday Trans. 2* **1972**, *68*, 86−100.
(23) Ge, M.-F.; Ma, C.; Xue, W. Acryloyl Chloride and Acryloyl Isocyanate (CH_2═$CHC(O)X$, X═Cl, NCO): A HeI Photoelectron Spectroscopy and Theoretical Study. *J. Phys. Chem. A* **2009**, *113*, 3108−3115.
(24) Alaee, M.; Hofstra, P.; Kirby, C.; Westwood, N. P. C.; He, I. Photoelectron Spectra of Unstable Boron Isocyanates; Electronic and Geometric Structures in the $BCl_x(NCO)_{3-x}$ Series. *J. Chem. Soc., Dalton Trans.* **1990**, 1569−1573.
(25) Alaee, M.; Livingstone, E. G.; Westwood, N. P. C. HeI Photoelectron, Mid-Infrared, and ab Initio Studies of the Unstable Fluoroisocyanatoboranes F_2BNCO and $FB(NCO)_2$. *J. Am. Chem. Soc.* **1993**, *115*, 2871−2876.
(26) Wang, W.; Yao, L.; Zeng, X.; Ge, M.-F.; Sun, Z.; Wang, D.; Ding, Y. Evidence of the Formation and Conversion of Unstable Thionyl Isocyanate: Gas-Phase Spectroscopic Studies. *J. Chem. Phys.* **2006**, *125*, 234303.
(27) Liu, F.; Zeng, X.; Wang, W.; Meng, L.; Zheng, S.; Ge, M. F.; Wang, D. Photoelectron Spectra and Electronic Structures of Some Chlorosulfonyl Pseudohalides. *Spectrochim. Acta, Part A* **2006**, *63*, 111−116.
(28) Zeng, X. Q.; Yao, L.; Ge, M. F.; Wang, D.-X. Experimental and Theoretical Studies on the Electronic Properties of Acetyl Pseudohalides $CH_3C(O)X$ (X═NCO, NCS and N_3). *J. Mol. Struct.* **2006**, *789*, 92−99.
(29) Zeng, X.; Ge, M.; Sun, Z.; Wang, D. Nitrosyl Isocyanate (ONNCO): Gas-Phase Generation and a HeI Photoelectron Spectroscopy Study. *Inorg. Chem.* **2005**, *44*, 9283−9287.
(30) Ramos, L. A.; Ulic, S. E.; Romano, R. M.; Vishnevskiy, Y. V.; Berger, R. J. F.; Mitzel, N. W.; Beckers, H.; Willner, H.; Tong, S.; Ge, M.; et al. Chlorodifluoroacetyl Isocyanate, $ClF_2CC(O)NCO$: Preparation and Structural and Spectroscopic Studies. *J. Phys. Chem. A* **2012**, *116*, 11586−11595.
(31) Chadwick, D.; Frost, D. C.; Herring, F. G.; Katrib, A.; Mcdowell, C. A.; Mclean, R. A. N. Photoelectron Spectra of Sulfuryl and Thionyl Halides. *Can. J. Chem.* **1973**, *51*, 1893−1905.
(32) Klapstein, D.; O'Brien, R. T. The He (I) Photoelectron Spectra of the Propenoyl Halides. *Can. J. Chem.* **1987**, *65*, 683−686.
(33) Erben, M. F.; Della Védova, C. O. Dramatic Changes in Geometry after Ionization: Experimental and Theoretical Studies on the Electronic Properties of Fluorocarbonyl (Mono-, Di-, and Tri-) Sulfur Compounds. *Inorg. Chem.* **2002**, *41*, 3740−3748.
(34) Niessen, W.; Fougere, S. G.; Janvier, D.; Klapstein, D. The Photoelectron Spectrum of Cyanoformyl Fluoride. *J. Mol. Struct.* **1992**, *265*, 133−142.
(35) Cooper, G.; Zarate, E. B.; Jones, R. K.; Brian, C. E. Absolute Oscillator Strengths for Photoabsorption, Photoionization and Ionic Photofragmentation of Sulphur Dioxide. II. The S 2p and 2s Inner Shells. *Chem. Phys.* **1991**, *150*, 251−261.
(36) Sze, K. H.; Brion, C. E.; Tronc, M.; Bodeur, S.; Hitchcock, A. P. Inner and Valence Shell Electronic Excitation of Dymethyl Sulfoxide by Electron Energy Loss and Photoabsorption Spectroscopies. *Chem. Phys.* **1988**, *121*, 279−297.
(37) Lessard, R.; Cuny, J.; Cooper, G.; Hitchcock, A. P. Inner-Shell Excitation of Gas Phase Carbonates and α,γ-dicarbonyl Compounds. *Chem. Phys.* **2007**, *331*, 289−303.
(38) Geronés, M.; Erben, M. F.; Romano, R. M.; Cavasso Filho, R. L.; Della Védova, C. O. Dissociative Photoionization of Methyl Thiochloroformate, $ClC(O)SCH_3$, Following Sulfur 2p, Chlorine 2p, Carbon 1s and Oxygen 1s Excitations. *J. Phys. Chem. A* **2012**, *116*, 7498−7507.
(39) Eland, J. H. D. The Dynamics of Three-Body Dissociations of Dications Studied by the Triple Coincidence Technique PEPIPICO. *Mol. Phys.* **1987**, *61*, 725−745.
(40) Eland, J. H. D.; Coles, L. A.; Bountra, H. Charge Separation Mass Spectrometry 1. Doubly-Ionized Perfluoro Compounds. *Int. J. Mass Spectrom. Ion Process.* **1989**, *89*, 265−285.